Modeling of Vacuum Insulating Glazing

Robert Hart, PE
Student Member ASHRAE

D. Charlie Curcija, PhD
Member ASHRAE

ABSTRACT

Windows with thermal resistance of R = 10 h·ft²·°F/Btu (U = 0.10 Btu/h·ft²·°F) or greater across the U.S. building stock could significantly reduce energy consumption (Arasteh 2006). Vacuum insulating glazing (VIG) is a promising technology that is capable of meeting the rigorous thermal performance requirements, but there is currently no simple method of evaluating its performance for research and development or certification.

In this work, the thermal transmittance (U-factor) of VIG is calculated with three methods: (1) analytical analysis using published correlations for modeling vacuum and pillar array conduction heat transfer; radiation heat transfer is solved explicitly using parallel plate theory; (2) two-dimensional finite element method computational heat transfer (2D FEM) where the pillar and vacuum space are replaced with an effective solid since 2D FEM cannot handle point thermal bridges such as pillars; and 3) three-dimensional finite volume numerical heat transfer modeling where pillar array conduction heat transfer and radiation heat transfer between surfaces in vacuum space are modeled to account for point thermal bridges such as pillars. The center-of-glass and edge-of-glass models from each method are compared to demonstrate a strong correlation between the methods and confirm applicability of representing vacuum space and pillar arrays using 2D FEM, the standard method of modeling and certifying windows and glazing.

INTRODUCTION

It is estimated that the implementation of "zero energy" windows with thermal resistance of R = 10 h·ft²·°F/Btu (U = 0.10 Btu/h·ft²·°F) performance across the U.S. building stock could reduce energy consumption $300 billion in the 20 years following these performance improvements (Arasteh 2006). Vacuum insulating glazing (VIG) for residential and commercial use is a promising technology that is capable of meeting the rigorous R-10 thermal performance requirements. While some VIG technology has been available in the Japanese and other markets as early as 1996, it has achieved minimal market penetration in the U.S. Some drivers for its low adoption include high costs, design features that restrict use in very hot or cold environments, and insulating performance (U = 1.2 W/m²·K center-of-glass [COG] by NSG) no greater than traditional triple glazing. New VIG products with claimed insulating performance down to U = 0.4 W/m²·K center-of-glass (far better than standard triple glazing), as well as the claimed ability to be installed in all U.S. climate regions, are being developed (Russo 2012; ENoB 2013; Jelle 2012; Eversealed 2013).

The COG thermal performance of VIG is well understood and the process for evaluation by analytical method is outlined in this work. The diversity of designs and complexities of edge-of-glass (EOG) heat flow though does not provoke an analytical model; therefore the three-dimensional finite volume computational method (3D FVM) is typically used for evaluation. 3D FVM models require trained and experienced users of specialized software and significant setup and evaluation effort. Such effort precludes the widespread use of these models in the fenestration industry and therefore the certification of windows using this technology. A simple

Robert Hart *is a scientific engineering associate and* ***D. Charlie Curcija*** *is a deputy group leader in the Windows & Envelope Materials Group, Lawrence Berkeley National Laboratory, Berkeley, CA.*

Published by ASHRAE 2013

and accurate method of evaluating whole window VIG performance using the U.S. fenestration industry standard two-dimensional finite element computational method (2D FEM) is proposed and evaluated in this work.

ANALYSIS

The analysis done in this study involves modeling procedures only. The thermal transmittance (U-factor) of VIG is calculated with three methods: (1) analytical analysis using published correlations for modeling vacuum and pillar array conduction heat transfer; radiation heat transfer is solved explicitly using parallel plate theory; (2) 2D FEM where the pillar and vacuum space are replaced with an effective solid since 2D FEM cannot handle point thermal bridges such as pillars; and (3) 3D FVM where pillar array conduction heat transfer and radiation heat transfer between surfaces in vacuum space are modeled to account for point thermal bridges such as pillars.

Analytical Method

The COG U-factor of VIG with support pillars is calculated analytically as a function of the surface resistances, glass resistance, and the vacuum gap resistance. The fundamental equations are presented here for completeness; the works of Collins (1991) and Corruccini (1959) should be reviewed for more detailed explanation of the methods.

$$U\text{-}factor = \frac{1}{R_o + 2 \cdot R_{glass} + R_{gap} + R_i} \tag{1}$$

where:

R_o = exterior surface resistance, $m^2 \cdot K/W$
R_i = interior surface resistance, $m^2 \cdot K/W$
R_{glass} = glass pane resistance, $m^2 \cdot K/W$
R_{gap} = vacuum gap resistance, $m^2 \cdot K/W$

The interior and exterior surface resistances are boundary conditions defined as a combination of convection and radiation resistance and listed in Table 3. The glass pane resistance is a function of total glass thickness and conductivity.

$$R_{glass} = \frac{t_{gl}}{k_{gl}} \tag{2}$$

where:

t_{gl} = glass thickness, m
k_{gl} = glass conductivity, W/m·K

The vacuum gap resistance is a function of the low-pressure gap conductance, the radiation conductance between glass panes, and the conductance of the support pillars between glass. The conductance of low-pressure gas is calculated using formula by Corruccini (1959). Equation 6 gives exact conductance of a pillar array, but pillar conductivity does not play a substantial role in overall heat transfer when the conductivity is equal to or higher than the conductivity of the glass pane. Therefore, a good approximation for common materials used in this technology can be made by ignoring the ratio of conductivities in the denominator of Equation 6.

$$R_{gap} = \frac{1}{C_{cond} + C_{rad} + C_{pa}} \tag{3}$$

$$C_{cond} = \left[\frac{\alpha_1 \cdot \alpha_2}{\alpha_2 + \alpha_1(1-\alpha_2)}\right] \cdot \left[\frac{\gamma+1}{\gamma-1}\right] \cdot \left[\frac{R}{4 \cdot \pi \cdot M \cdot (T_{1c} + T_{2c})}\right]^{\frac{1}{2}} \cdot P \tag{4}$$

$$C_{rad} = \frac{\sigma}{\varepsilon_1^{-1} + \varepsilon_2^{-1} - 1} \cdot \left[\frac{T_1^4 - T_2^4}{T_1 - T_2}\right] \tag{5}$$

$$C_{pa} = \frac{2 \cdot \kappa_{gl} \cdot a}{l^2 \cdot \left(1 + \frac{2 \cdot \kappa_{gl} \cdot h}{\kappa_p \cdot \pi \cdot a}\right)} \tag{6}$$

where:

C_{cond} = conductance of low pressure gas between glass, $W/m^2 \cdot K$
C_{rad} = radiation conductance between glass panes, $W/m^2 \cdot K$
C_{pa} = conductance of pillar array between glass panes, $W/m^2 \cdot K$
α_1, α_2 = accommodation coefficients of the gas molecules. Dependent on the temperature, surface conditions, etc. For the present configuration and conditions, $\alpha_1, \alpha_2 \cong 0.5$. If conservative, 1.0 could be used.
γ = specific heat ratio, $\gamma_{air} = 1.40$
R = universal gas constant, $R = 8{,}314.462175$ J/mol·K
M = molecular weight, $M_{air} = 28.97$ mol/g
T_{1c} = exterior temperature, K
T_{2c} = interior temperature, K
P = gas pressure, N/m^2
σ = Stefan-Boltzmann constant 5.67×10^{-8} $W/m^2 \cdot K^4$
ε_1 = emissivity of the first facing glass surface, –
ε_2 = emissivity of the second facing glass surface, –
T_1 = temperature of the first facing glass surface, K
T_2 = temperature of the second facing glass surface, K
a = pillar radius, m
h = pillar height, m
k_p = pillar conductivity, W/m·K
l = pillar spacing, m

Two-Dimensional Finite Element Method

2D FEM is used to solve the conductive heat-transfer equation for two-dimensional analysis. The quadrilateral mesh is automatically generated. Refinement is performed in accordance with section 6.3.2b of ISO 15099 (ISO 2003). The energy error norm is less than six percent in all cases, where it has been shown that energy error norm of 10% or less correlates to an error of less than one percent in the total thermal transmittance of the object(s) being modeled. More information on the thermal simulation program algorithms can be found in Finlayson (1998) and Carli (2006).

Center-of-glass. Modeled COG geometry for 2D FEM makes use of symmetry as shown in Figure 1. 2D FEM cannot handle point thermal bridges such as pillars, which are properly modeled only in three-dimensional space, therefore, the pillars and vacuum space are replaced with an effective solid whose properties are calculated for each configuration by Equation 3.

Edge-of-glass. Modeled EOG geometry for 2D FEM analysis makes use of symmetry as shown in Figure 2. The vacuum space from the edge-of-glass to the first pillar is replaced with an effective solid whose properties are calculated for each configuration by Equation 3 with the conductance of the pillars set to zero. Starting at first pillar, the vacuum space is modeled similar to the COG, with an effective solid whose properties are calculated for each configuration by Equation 3. The influence of edge conduction in the geometries modeled becomes negligible after the third pillar, as is shown later.

Due to the relative high conductivity of the edge compared to COG in current VIG design, an exposed edge region would exhibit very high heat transfer rates that are difficult to measure in real systems due to condensation and frost build-up. For these reasons the edge is modeled as covered by a 12.5 mm square wood block on the interior and exterior sides of the VIG. This technique effectively reduces heat transfer through the edge region to a magnitude in line with a VIG installed into a window frame. A similar approach is taken by Simko (1996).

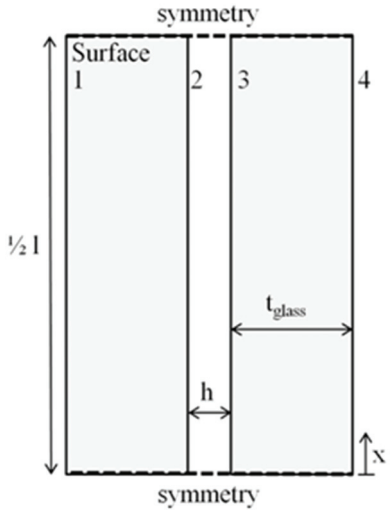

Figure 1 *COG model geometry for 2D FEM analysis (not to scale).*

Three-Dimensional Finite Volume Method

3D FVM is used to solve the coupled heat and fluid-flow equations for three-dimensional analysis. Conduction, convection, and radiation are simulated numerically. Three-dimensional analysis is necessary to account for the non-continuous pillar shapes between glass. Because the Navier-Stokes fluid equations typically used by commercial solvers are invalid at the low pressures seen in VIGs, two alternative methods are used to approximate the gap conductance: (1) The "solid" model, where the vacuum gap is defined as a solid with a combined fluid and radiation conductivity solved by the analytical methods of Equation 3; (2) The "radiation" model, where the vacuum gap is defined as a fictitious fluid and radiation is solved for explicitly. In both methods, pillars are modeled with their actual geometry.

The semi-implicit method for pressure-linked equations consistent (SIMPLEC) was used to model the interaction between pressure and velocity. The energy and momentum variables at cell faces were found by using the

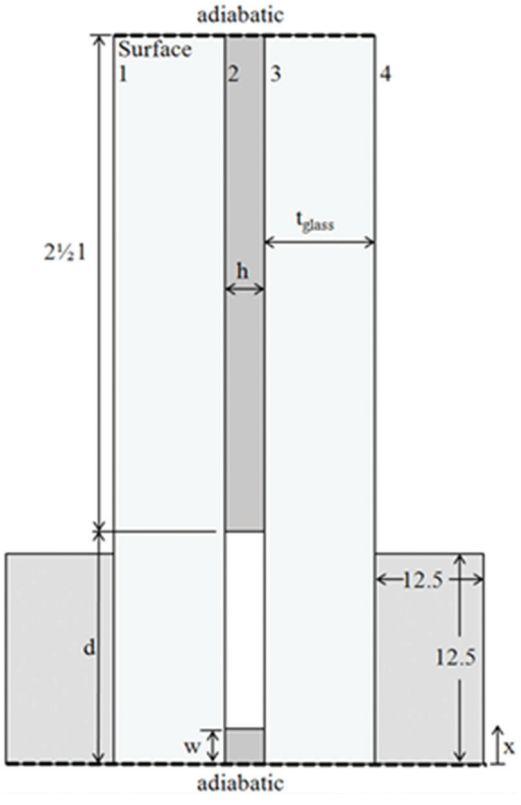

Figure 2 *EOG model geometry for 2D FEM analysis (not to scale).*

Quadratic Upstream Interpolation for Convective Kinetics (QUICK) scheme. The commercial software used solves central differences to approximate diffusion terms and relies on the PREssure STaggering Option scheme (PRESTO) to find the pressure values at the cell faces. Convergence is determined by checking the residuals for energy and ensuring that they are lower than 1E-13. Radiation heat transfer is included in the simulations through use of Surface to Surface (S2S) radiation model, which calculates the energy exchange between surfaces taking into account their size, separation distance, and orientation using a geometric function called *view factor*. The S2S model ignores absorption, emission, and scattering phenomena in the vacuum cavity. The internal cavity walls were assumed to be diffuse gray. The meshing program automatically generated meshes. Mesh refinement was done at pillars and edge seals to ensure acceptable mesh density and orthogonal quality.

Center-of-glass. Modeled COG geometry used for 3D FVM analysis makes use of symmetry as shown in Figure 3. This geometry is referred to as a *¼ pillar model* as it utilizes symmetry around ¼ of a pillar as shown in section (B). Additional model geometries were tested, including a full pillar and a 3 × 3 grid of pillars. The variation between the three models in all cases was less than 0.50 percent.

Edge-of-glass. Modeled EOG geometry used for 3D FVM analysis makes use of symmetry as shown in Figure 4. This model uses the same ¼ pillar symmetry as the COG model but extends three and one-half pillars from the edge. Additional models geometries were generated, including single pillar and 5 pillar models. The influence of edge conduction in the geometries modeled becomes negligible after the third pillar. As in 2D FEM, an exposed edge region would exhibit very high heat transfer rates, so the edge model is covered by a 12.5 mm square wood block on the interior and exterior sides of the EGU.

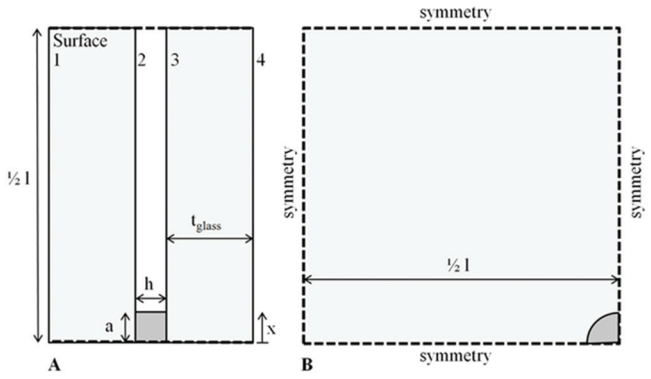

Figure 3 *COG model geometry for 3D FVM analysis (not to scale).*

Model Parameters

Table 1 lists the model dimension ranges used for this study. The minimum (min) and maximum (max) are selected to represent the range of expected design. Thermal performance sensitivities are determined by varying material properties and model dimensions. Table 2 displays the material properties for each component used in the numerical simulations. Base material data is obtained from NFRC 101 (2010). Min and max values are selected based on available materials and to properly demonstrate sensitivities.

Boundary conditions used in the 3D FVM and 2D FEM simulations are shown in Table 3. The outdoor and indoor boundary conditions use a fixed combined convection and radiation coefficient. Fixed boundary conditions are used, as opposed to temperature dependent conditions such as ASHRAE, to simplify modeling. The methods outlined are valid for fixed and variable boundary conditions.

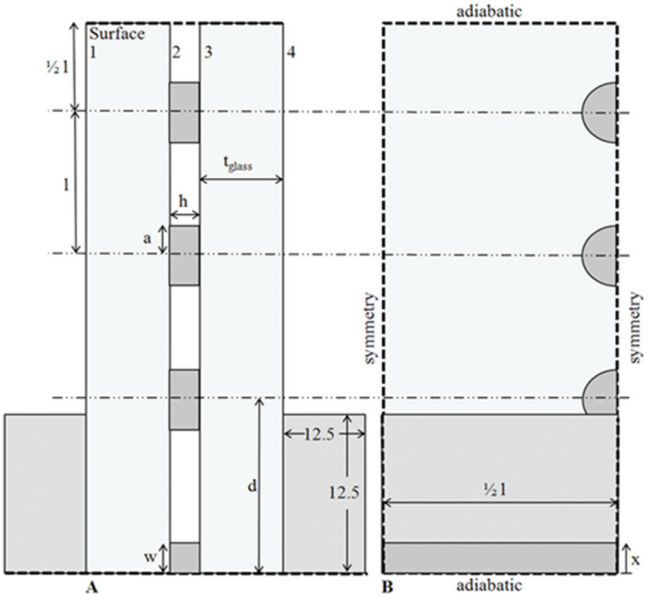

Figure 4 *EOG model geometry for 3D FVM analysis (not to scale).*

Table 1. Model Dimensions

Dimension	Variable	Base (mm)	Min (mm)	Max (mm)
Pillar radius	*a*	0.5	0	1
Vacuum gap	*h*	0.13	0.05	1
Glass thickness	t_{glass}	5.7	2.7	7.2
Pillar spacing	*l*	50.8	25	125
Pillar to edge of glass	*d*	25	10	50
Edge seal thickness	w	7.2	0	10.5

RESULTS AND DISCUSSION

Center-of-Glass (COG)

Figure 5 shows the temperature of each glass surface at a specified distance, *x*, from the center of a pillar (see Figure 3). To account for the localized pillar effects, this model is performed using 3D FVM. The external surfaces 1 and 4 show approximately one Kelvin temperature changes over the length of the model. This means that using an area weighted equivalent conductance (2D FEM) has little impact on external surface temperatures. The internal surfaces 2 and 3 reach 95% of their total temperature change at 5.4 and 6.1 mm, respectively, from the pillar center, meaning the thermal bridging effect of the pillar is a radius of approximately 6.5 mm for the configurations used in this study. A similar plot of the 2D FEM model shows constant temperatures along *x* since Equation 3 averages pillar heat transfer over the entire vacuum volume.

Table 2. Conductivity and Emissivity of Modeled Materials

	Conductivity (W/m·K)			Emissivity		
Component	Base	Min	Max	Base	Min	Max
Outside glass	1	–	–	(1) 0.84 (2) 0.02	(1) — (2) 0.02	(1) — (2) 0.84
Inside glass	1	–	–	(3) 0.84 (4) 0.84	(3) — (4) —	(3) — (4) —
Pillar	16	–	–	0.9	–	–
Edge seal	1	0.01	100	0.9	–	–
Wood	0.14	–	–	0.9	–	–

Table 3. Boundary Conditions Used in the Simulations

Boundary Condition	Value	Units
Indoor temperature	293.15	K
Outdoor temperature	255.15	K
Density of heat flow rate of incident solar radiation on surface	0	W/m^2
Combined convection and radiation surface coefficient of heat transfer for the indoor section (surface 4)	7.6	W/m^2·K
Combined convection and radiation surface coefficient of heat transfer for the outdoor section (surface 1)	30.0	W/m^2·K
Density of heat flow rate at lines of symmetry	0	W/m^2

Sensitivities to changes in variables. Analytical, 2D FEM, and 3D FVM models are compared for twenty-six cases of COG U-factor. The 3D FVM radiation method is used as the base for comparison since the model is calculated on the most fundamental basis and has been shown in previous studies to agree well with measurements (Simko 1996). Summarized sensitivity results are presented in Table 4. These results show the four models solve for total thermal transmittance within ~0.01 W/m^2·K, or 2 percent, of each other for all parameter variations in this study. The results for the range of parameters chosen confirm that 2D FEM is an accurate alternative to 3D FVM.

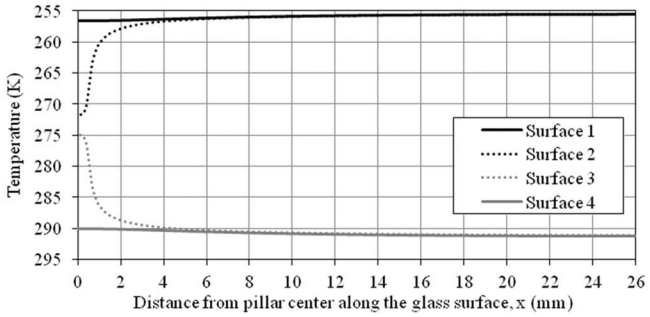

Figure 5 *COG surface temperature distribution from 3D FVM.*

Table 4. COG Thermal Transmittance (U-Factor) Using Four Solution Methods

	3D FVM "Radiation" (W/m^2·K)		3D FVM "Solid" (W/m^2·K)		2D FEM (W/m^2·K)		Analytical (W/m^2·K)	
Parameter	Min U	Max U	Average Δ*U*	Average Δ%	Average Δ*U*	Average Δ%	Average Δ*U*	Average Δ%
Vacuum Gap	0.422	0.449	–0.002	–0.6%	–0.010	–2.3%	–0.010	–2.3%
Pillar Radius	0.097	0.766	–0.001	–0.2%	–0.005	–1.1%	–0.005	–1.1%
Pillar Spacing	0.154	1.313	–0.001	–0.2%	–0.001	–1.4%	–0.001	–1.4%
Surface 2 Emissivity	0.446	2.215	–0.020	–1.3%	–0.026	–2.1%	–0.026	–2.1%
Vacuum Pressure	0.441	0.866	–0.001	–0.2%	–0.009	–1.7%	–0.009	–1.7%

The 3D FVM radiation model accounts for localized radiation effects within the radius of pillar thermal bridging while the 3D FVM solid, 2D FEM, and analytical models do not. This results in a slight divergence of the solved thermal transmittance when surface emissivity is increased, as can be seen in Figure 6. The best agreement between 3D FVM and 2D FEM is therefore at low surface 2 emissivity.

Edge-of-Glass (EOG)

NFRC 100 considers all glazed vision areas within 63.5 mm of any part of the frame EOG (NFRC 2010). In order for this assumption to be accurate, and not overestimate the whole window U-factor, the penetration length of thermal effects from frame and end of glazing must be less than 63.5 mm. To determine the penetration length of the EOG effects into the VIG unit, the EOG was modeled with 3D FVM to six pillars in length. The results showed the temperature change on surfaces 1 and 4 at a distance halfway between pillars 3 and 4 is less than 1 percent different from the temperature between pillars 5 and 6. This shows that the edge effect has stabilized by the third pillar and a 3.5 pillar model is used for the remainder of the EOG calculations.

For all combinations of edge seal conductance, pillar spacing, and distance to first pillar, the external surfaces 1 and 4 reach 95% of their total temperature change at approximately 50 mm from the edge, meaning the thermal bridging effect of the edge is within the NFRC EOG for the configurations used in this study. The localized thermal effects of pillars cannot be solved for with a 2D FEM model. The surface temperatures though do closely match those from 3D FVM models at locations outside of pillar effects. Figure 7 compares the EOG glass surface temperatures of each glass surface at a specified distance, x, from the EOG (see Figures 2 and 4) of 2D FEM and 3D FVM models on a unit with surface 2 emissivity of 0.02.

Sensitivities to changes in variables. Since the goal of this study is to account for total heat flow, the EOG distance in this study is longer than 63.5 mm and the reported U-factors are based on the total interior length of the EOG model (includes heat flow though the wood block). Therefore, these models are not directly comparable to typically reported EOG values in standards.

2D FEM, 3D FVM radiation and 3D FVM solid model results are compared for eleven cases of EOG U-factor. Due to the complexity of the edge seal, an entirely analytical solution for the EOG is not attempted. As in the COG calculations, 3D FVM radiation method is used as the base for comparison since the model is calculated on the most fundamental basis.

When pillars are located close to the EOG, they can become a localized conduction path to the frame that is ignored in the area weighted (2D FEM) calculations. The total thermal transmittance though shows negligible divergence between 2D FEM and 3D FVM. Summarized results are presented in Table 5. These results show the three models solve for total thermal transmittance within 0.01 W/m^2·K, or less than 1.3%, of each other for the three parameter variations in this study. The results for the range of parameters chosen confirm that 2D FEM is an accurate alternative to 3D FVM.

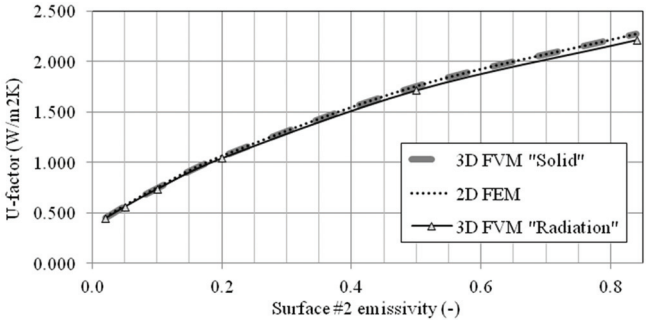

Figure 6 *COG sensitivity to surface 2 emissivity by modeling method.*

CONCLUSION

The center-of-glass (COG) thermal performance of VIG is well understood and simple analytical evaluation has been shown in previous work, and again in this study, to match 3D FEM approximations within 2.3% of total thermal transmittance. The diversity of designs and complexities of EOG heat flow though does not allow for a simple analytical model; therefore difficult and time consuming 3D FVM models are typically used for evaluation. The 2D FEM alternative to such models outlined in this work requires far less computational effort and produces similar total thermal transmittance approximations, within 1.3% of 3D FVM. Concerns regarding EOG length and localized pillar conductance are shown to have little impact on total performance and therefore can be neglected in 2D FEM. This alternative approach will allow for the widespread use of these models in the fenestration industry and therefore the certification of windows using this technology.

ACKNOWLEDGMENTS

This work was supported by the assistant secretary for Energy Efficiency and Renewable Energy, Building Technologies Program, of the U.S. Department of Energy under Contract no. DE-AC02-05CH11231.

REFERENCES

Arasteh, D., S. Selkowitz, J. Apte, and M. LaFrance. Zero Energy Windows. ACEEE Summer Study on Energy Efficiency in Buildings. 2006

Carli. 2006. Conrad 5 & Viewer 5 Technical and Programming Documentation. Carli, Inc. Technical Report. June 20, 2006.

Collins, R.E., and Robinson, S.J. 1991. Evacuated Glazing. *Solar Energy*. Vol. 47, No. 1, pp. 27–38.

Collins, R.E., and Fischer-Cripps, A.C. 1991. Design of Support Pillar Arrays in Flat Evacuated Windows. Aust. *J. Phys.*

Corruccini, R.J. 1959. Gaseous Heat Conduction at Low Pressures and Temperatures. *Vacuum*. Vol. 7–8, pp.19–29

ENoB (Research for Energy Optimized Buildings). Next Step: Vacuum insulation glass. Retrieved April, 17 2013. http://www.enob.info/en/new-technologies/projects /details/next-step-vacuum-insulation-glass/

Eversealed Windows. Technically Speaking Retrieved April 17, 2013. http://www.eversealedwindows.com/

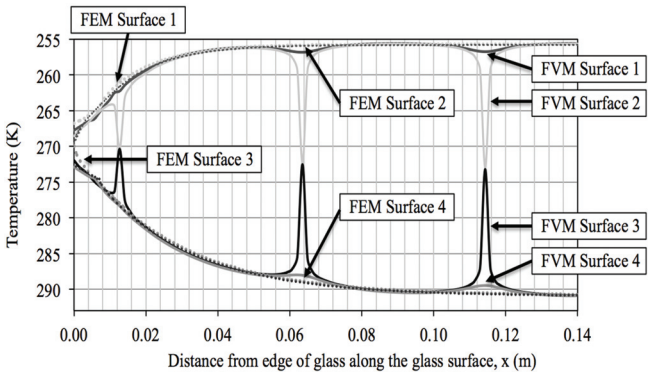

Figure 7 *EOG surface temperature distribution.*

Finlayson, E., R. Mitchell, D. Arasteh, C. Huizenga, and D. Curcija. 1998. *THERM 2.0*: Program description. A PC program for analyzing the two-dimensional heat transfer through building products. Berkeley, CA: University of California.

ISO 15099. 2003. *Thermal Performance o Windows, Doors and Shading Devices—Detailed Calculations*. Geneva, Switzerland: International Organization for Standardization.

Jelle, B.P., A. Hynd, A. Gustavsen, D. Arasteh, H. Goudey, and R. Hart. 2012. Fenestration of today and tomorrow: A state-of-the-art review and future research opportunities. *Solar Energy Materials and Solar Cells*, Vol. 96, pp 1–28.

National Fenestration Rating Council. 2010. NFRC-100-2010E0A1. *Procedure for Determining Fenestration Product U-factors*.

National Fenestration Rating Council. 2010. NFRC-101-2010E2A7. *Procedure for Determining Thermophysical Properties of Materials For Use in NFRC-Approved Software Programs*.

Russo, A. May 1, 2012. New Glass Technologies Promise More Energy Savings. *Window and Door*. Retrieved April, 17 2013. http://www.windowanddoor.com/article/may-2012/new-glass-technologies-promise-more-energy-savings

Simko, T.M. 1996. Heat Transfer Processes and Stresses in Vacuum Glazing. PhD thesis. The University of Sydney.

Table 5. Table 5. EOG Thermal Transmittance (U-Factor) Using Three Solution Methods

	3D FVM Radiation Model (W/m²·K)		3D FVM Solid Model (W/m²·K)		2D FEM (W/m²·K)	
Parameter	**Min *U***	**Max *U***	**Average Δ*U***	**Average % difference**	**Average Δ*U***	**Average % difference**
Glass Thickness, t_{glass}	0.835	0.988	–0.001	–0.1%	0.003	0.3%
Pillar from EOG, *d*	0.871	0.998	–0.001	–0.1%	0.004	0.5%
Edge Seal Conductance	0.652	0.963	–0.001	–0.1%	0.010	1.3%